Small potassium ion channel proteins encoded by chlorella viruses

Ming Kang*, Anna Moroni†‡, Sabrina Gazzarrini†, Dario DiFrancesco‡§, Gerhard Thiel¶, Maria Severino†, and James L. Van Etten*‖**

*Department of Plant Pathology and ‖Nebraska Center for Virology, University of Nebraska, Lincoln, NE 68583-0722; Departments of †Biology and Consiglio Nazionale delle Ricerche Istituto di Biofisica and §Biomolecular Sciences and Biotechnology, Università degli Studi di Milano, Via Celoria 26, 20133 Milano, Italy; ‡Istituto Nazionale di Fisica della Materia, Unità di Milano–Università, Via Celoria 16, 20133 Milano, Italy; and ¶Institute of Botany, Darmstadt University of Technology, 64287 Darmstadt, Germany

This contribution is part of the special series of Inaugural Articles by members of the National Academy of Sciences elected on April 29, 2003.

Contributed by James L. Van Etten, November 25, 2003

Kcv, a 94-aa protein encoded by *Paramecium bursaria* chlorella virus 1, is the smallest known protein to form a functional potassium ion channel and basically corresponds to the "pore module" of potassium channels. Both viral replication and channel activity are inhibited by the ion channel blockers barium and amantadine but not by cesium. Genes encoding Kcv-like proteins were isolated from 40 additional chlorella viruses. Differences in 16 of the 94 amino acids were detected, producing six Kcv-like proteins with amino acid substitutions occurring in most of the functional domains of the protein (N terminus, transmembrane 1, pore helix, selectivity filter, and transmembrane 2). The six proteins form functional potassium selective channels in *Xenopus* oocytes with different properties including altered current kinetics and inhibition by cesium. The amino acid changes together with the different properties observed in the six Kcv-like channels will be used to guide site-directed mutations, either singularly or in combination, to identify key amino acids that confer specific properties to Kcv.

K^+ channel structure–function | Kcv | PBCV-1

Paramecium bursaria chlorella virus (PBCV-1) (genus *Chlorovirus*, family Phycodnaviridae) is the prototype of a family of large double-stranded DNA-containing plaque-forming viruses that infect certain isolates of unicellular eukaryotic chlorella-like green algae (1, 2). Sequencing the PBCV-1 330-kb genome revealed an ORF (ORF A250R) encoding a small protein of 94 amino acids with similarities to the family of two transmembrane domain potassium ion (K^+) channel proteins. The similarities include the putative transmembrane (TM) topology and a pore region connecting the two TM domains. The predicted pore region of the protein contains the selectivity filter amino acid sequence ThsTvGFG, characteristic of K^+ channels. Peculiar to the PBCV-1 protein, named Kcv, is a short cytoplasmic N terminus of 12 amino acids and the absence of a cytoplasmic C terminus. Thus, Kcv represents the "pore module," a membrane–pore–membrane structure common to all K^+ channels.

Expression studies established that Kcv forms a functional K^+ channel in several heterologous systems, including *Xenopus* oocytes (3) and mammalian human embryonic kidney 293 (4) and Chinese hamster ovary (5) cells. The K^+ selectivity and sensitivity to channel blockers of the Kcv channel resemble those of more complex K^+ channels from eukaryotic organisms, suggesting a conserved pore architecture. Kcv even exhibited some voltage dependency, indicating a moderate inward rectification. Because of its small size, Kcv is a model protein for understanding structure–function relationships, and it may have the minimal structural requirement for forming a functional K^+ selective channel.

The relationship among protein structure and function has been intensively studied in K^+ channels by using site-directed mutagenesis or directed evolution strategies in combination with biophysical analyses of channel function (e.g., refs. 6–8). These studies have provided a basic understanding of many structure–function relationships, several of which have been confirmed by crystal structures of K^+ channel proteins (9, 10). However, mutation analysis of proteins is never complete. It is nearly impossible to exchange each amino acid in a protein with all possible amino acids. Furthermore, when functional changes involve the synergistic action of more than one amino acid, e.g., two amino acids, a combination of $>10^{11}$ possibilities exists in a protein the size of Kcv. Because libraries of this size cannot be synthesized easily, structurally important interactions may evade detection by conventional mutagenesis strategies.

This article describes a previously undescribed approach for uncovering structure–function relations in a K^+ channel by using the chlorella viruses. Functional studies have established that the Kcv channel is probably required for virus PBCV-1 replication (3, 11). Separate studies suggest that the chlorella viruses have a long evolutionary history (2, 12). Consequently, amino acid sequences of homologous proteins encoded by the viruses differ by as much as 25% (2). Because of these properties, we have isolated genes encoding Kcv-like proteins from 40 additional chlorella viruses; these viruses come from freshwater collected throughout the world. In total, differences in 16 of the 94 Kcv amino acids were obtained, resulting in six Kcv-like proteins. Amino acid differences occurred in all of the Kcv functional domains. The six Kcv-like proteins, which differ from PBCV-1 Kcv by 4–12 amino acids, produced K^+ selective currents in *Xenopus* oocytes with altered biophysical properties, e.g., current kinetics, voltage dependency, and inhibition by Cs^+.

Materials and Methods

Viruses and Culture Conditions. The growth of the host alga, *Chlorella NC64A*, on MBBM medium, the plaque assay, the production of the viruses, and the isolation of virus DNAs have been described (13–15). Plaque inhibition studies were conducted as follows. Actively growing *Chlorella NC64A* cells in liquid culture were infected at a multiplicity of infection of five at the same time inhibitors were added. The mixtures were incubated at 25°C for 2 h with moderate shaking, briefly centrifuged to remove unattached virus, and then plaqued for infective centers on inhibitor-containing media as described previously (14).

Abbreviations: TM, transmembrane; PBCV-1, *Paramecium bursaria* chlorella virus; Ii, instantaneous current; *I–V*, current/voltage.

Data deposition: The sequences reported in this paper have been deposited in the GenBank database (accession nos. AY338212–AY338225).

See accompanying Biography on page 5315.

**To whom correspondence should be addressed. E-mail: jvanetten@unlnotes.unl.edu.

© 2004 by The National Academy of Sciences of the USA

PCR. Single virus plaques were excised from plates and suspended in 100 μl of 50 mM Tris·Cl buffer, pH 7.8. The suspensions were shaken for 10 min, and then the samples were centrifuged at low speed (1,400 $\times$ *g*) for 1 min. Viruses in the supernatant were disrupted and virus DNA denatured by boiling for 10 min before PCR amplification by using the following oligonucleotide primers: 5′ primer CGGGAATTCATGTTAGTGTTTAGTA-AATTTCT and 3′ primer TCTCTCGAGTCATAAAGTTA-GAACGATGAAG. The PCR contained 3 μl of denatured virus DNA, 100 pmol of each primer, 10 mM of each dNTP, 10 units of Vent DNA polymerase (New England Biolabs), and 5 μl of 10$\times$ thermolpol buffer in a 50-μl reaction volume. Amplification was carried out by using 35 cycles of 94°C for 1 min, 58°C for 1 min, and 72°C for 1.5 min. PCR fragments were cloned into pGEM7Z at *Xho*I and *Bam*HI sites and sequenced by using the 5′ T7 primer or the 3′ Sp6 primer.

To sequence the 5′ and 3′ ends of selected *kcv* genes, viral DNA restriction fragments containing the *kcv* gene were identified by hybridization; the fragments were self-ligated and subjected to inverse PCR. The upstream primer (5′-GATGC-CTTTTTGTCCGGGTTTGCAACAGA-3′) and the downstream primer (5′-TTCGGAACGACACACTC-3′) were designed from conserved nucleotide sequences present in all of the viruses. Fifty-microliter reactions contained 1 μl of template, 100 pmol of primer, 10 mmol of each dNTP, 4 units of BIO-X-ACT DNA polymerase (Bioline, London), 5 μl of 10$\times$ reaction buffer, 10 μl of 5$\times$ Specificity Enhancer (Bioline), and 2 mmol of $MgCl_2$.

Expression of the *kcv* Genes in Oocytes. Kcv cDNA was cloned into pSGEM vector (a modified version of pGEM-HE, courtesy of M. Hollmann, Max Planck Institute for Experimental Medicine, Göttingen, Germany). We prepared RNA by T7 polymerase transcription and injected it (20–40 ng per oocyte) into *Xenopus laevis* oocytes prepared according to standard methods (3). Measurements were performed 2–4 days after injection.

Electrophysiology. A two-electrode voltage clamp (Gene clamp 500, Axon Instruments, Foster City, CA) was used to record K^+ currents from oocytes. Electrodes were filled with 3 M KCl and had a resistance of 0.2–0.8 MΩ (in 50 mM KCl). The oocytes were perfused at room temperature with a standard bath solution containing 50 mM KCl (or RbCl, NaCl, LiCl, CsCl, as indicated in Figs. 4–6 legends and text), 1.8 mM $CaCl_2$, 1 mM $MgCl_2$, and 5 mM Hepes, adjusted to pH 7.4 with KOH, at a rate of 2 ml·min^{-1}. Mannitol was used to adjust the osmolarity of the solution to 215 mosmol.

The standard clamp protocol consisted of steps from the holding voltage of -20 mV to voltages in the range $+80$ mV to -160 mV; tail currents were measured at -80 mV. Instantaneous and steady-state currents were sampled after 10 ms and at the end of the voltage step (usually 800 ms), respectively.

Ion Permeability. Permeability ratios (P_B/P_A) were calculated by using the following equation (16):

$$\Delta E_{rev} = E_{rev,B} - E_{rev,A} = RT/zF \ln P_B[B]_o/P_A[A]_o.$$

E_{rev} is the value in mV of the current reversal potential measured in the presence of 50 mM monovalent cation (either $[A]_o$ or $[B]_o$ in the external solution; R is the gas constant, 8.3145 V C mol^{-1}·K^{-1}; T is the absolute temperature T(K), 273.15 + T(°C); z is the ion charge; and F is Faraday's constant, 9.6485 $\times$ 10^4 C·mol^{-1}.

Other Procedures. DNA hybridization procedures have been described previously (17). DNAs were sequenced at the University of Nebraska Center for Biotechnology DNA sequencing core facility. DNA, RNA, and protein sequences were analyzed with the University of Wisconsin Genetics Computer Group Version 10.1 package of programs (GENETICS COMPUTER GROUP, 2000). The *kcv* gene sequences are in the GenBank database under accession numbers AY338212–AY338225.

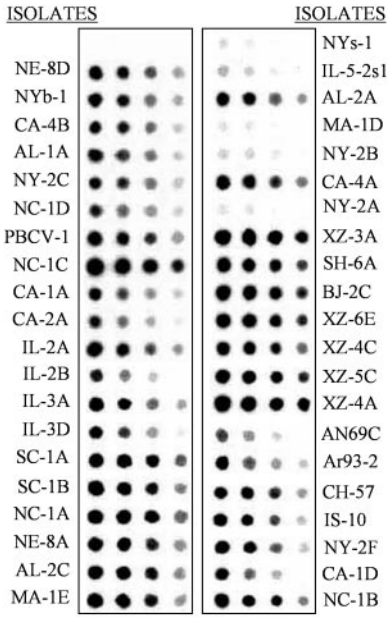

Fig. 1. The *kcv*-like gene is ubiquitous in chlorella viruses. Hybridization of the PBCV-1 *kcv* gene to DNA isolated from 40 viruses that infect *Chlorella NC64A*. The spots contain 1.0, 0.5, 0.25, and 0.125 μg of DNA (left to right).

Results

Isolation of the *kcv* Gene from the Chlorella Viruses. To determine whether the *kcv* gene is common in the chlorella viruses, genomic DNAs from 40 chlorella viruses from diverse geographical regions (see table 1 in ref. 18) were hybridized to a PBCV-1 *kcv* probe (Fig. 1). The probe hybridized strongly to 35 of the 40 viruses. Five viruses (NYs-1, IL-5–2sl, MA-1D, NY-2B, and NY-2A) hybridized poorly with the probe. Because the strength of the hybridization signal differed among the viruses, we expected to find significant nucleotide substitutions in the *kcv* genes.

Amplification of viral DNAs with PCR primers designed from the PBCV-1 *kcv* sequence produced a PCR product of the expected size, 285 nt, from 37 of the viruses. The 37 PCR products were sequenced, and 11 distinct DNA patterns were obtained. Because the PCR primers hybridized to eight codons at each end of the *kcv* genes, small nucleotide differences in these two regions of the gene would be concealed. To look for changes in these regions, DNA restriction fragments containing the *kcv* gene from 13 of these 37 viruses were identified by hybridization with the *kcv* gene, eluted from the gels, self-ligated, subjected to inverse PCR, and the product was sequenced.

The *kcv* gene was identified in the three remaining viruses (MA-1D, NYs-1, and NY-2A) by hybridizing the PBCV-1 *kcv* gene at low stringency to restriction digests of the viral DNAs. DNA fragments that hybridized with the probe were cloned and sequenced. These experiments identified a putative *kcv* gene in each of the 40 viruses.

Diversity of the *kcv* Gene in the Chlorella Viruses. The nucleotide sequence of the PCR products and the cloned fragments verified that all 40 viruses contained a 94-codon-containing *kcv* gene. The sequence of the *kcv* genes produced 13 patterns (Fig. 2). The

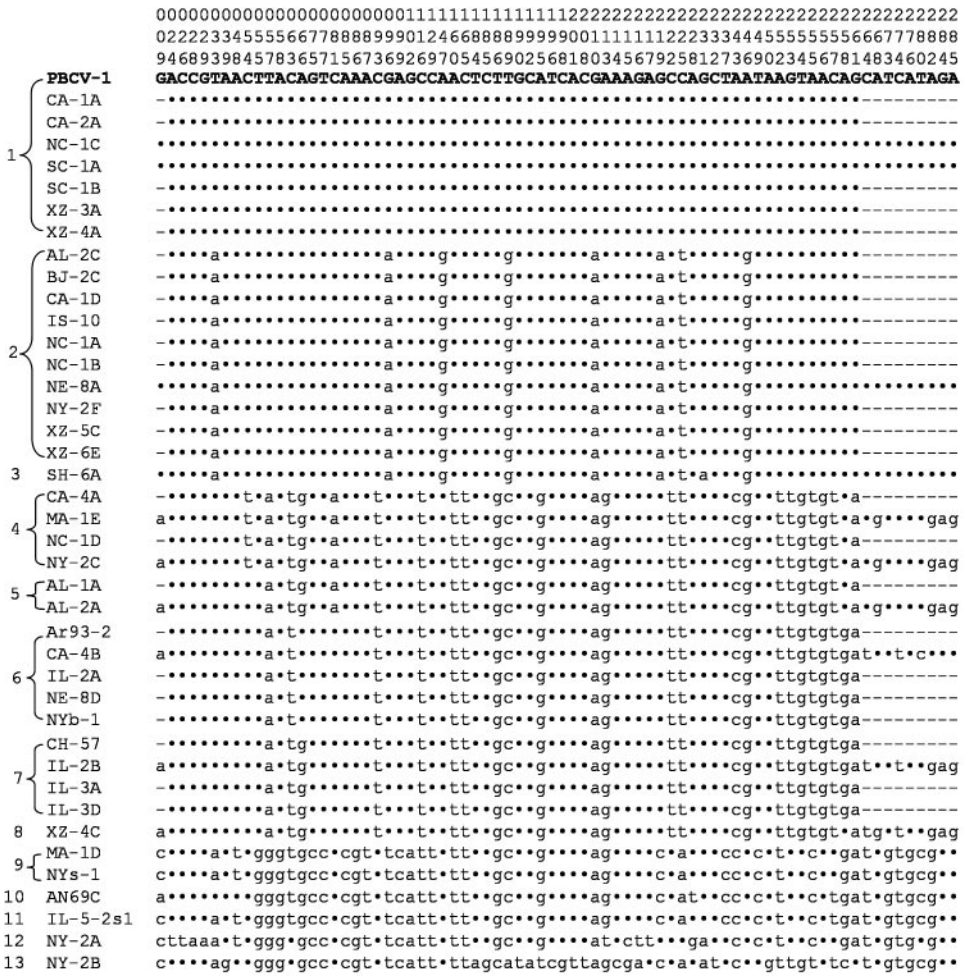

Fig. 2. Diversity of *kcv* gene among chlorella viruses. Differences in the 285 nucleotide coding regions (including stop codons) of the *kcv* gene from 40 chlorella viruses as compared with the PBCV-1 *kcv* gene are shown. Only the sites that had a nucleotide change, numbered at the top, are listed. A dot indicates no change, and a dash means not determined.

DNA sequences from seven of the viruses were identical to that of PBCV-1 *kcv*. Six of the 13 *kcv* nucleotide sequences occurred in a single virus. To eliminate possible PCR-produced errors, all *kcv* genes were isolated and sequenced a second time. In total, 74 or 26% of the 285 nucleotides differed from the PBCV-1 *kcv* sequence. Forty-five percent or 61% of these 74 nucleotide substitutions occurred in the third position of the codon. The virus NY-2B *kcv*, with 53 nucleotide substitutions, differed the most from the PBCV-1 *kcv* sequence. The *kcv* gene from 12 viruses terminated with a TGA codon and with a TAG codon in five viruses.

Not surprisingly, fewer changes occurred in the amino acid sequences of the Kcv protein. Collectively, substitutions occurred in 16 of the 94 amino acid positions (Fig. 3*A*; only one representative of each protein is shown). Nine of the 16 amino acid substitutions occur in the TM domains of the protein; 12 of the 16 changes reflect conservative amino acid substitutions in the protein. Four amino acids, Thr, Val, Met, and Ile, occur at position 86.

Including PBCV-1 Kcv, the virus proteins were classified into seven groups (Fig. 3*A*). The Kcv protein from 19 viruses had the same amino acid sequence as PBCV-1 Kcv. The Kcv protein from 12 viruses differed by four amino acids from PBCV-1 Kcv (represented by virus CA-4B in Fig. 3*A*); two groups had two members. The amino acid sequences of the Kcv protein from viruses MA-1D and NYs-1 were identical and differed by five amino acids from PBCV-1 Kcv, whereas the Kcv protein from viruses AN69C and IL-5–2sl were identical and differed by six amino acids from the PBCV-1 sequence. Two viruses have amino acid substitutions that might influence the basic functional or structural properties of the Kcv protein. (*i*) The eight amino acid residue K^+ channel pore signature sequence in virus NY-2B differs by two amino acids from all other Kcv proteins, i.e., the ThsTvGFG pore domain is changed to ThsTIGLG. (*ii*) Virus NY-2A has two amino acid substitutions in a potential phosphorylation site at residues 7–10. The TRTE sequence, which is present in the Kcv protein encoded by all of the other viruses, is changed to MKTE. However, this site is probably not a critical phosphorylation site, because a Thr-9Ala substitution in the PBCV-1 Kcv protein did not alter K^+ conductance (4). No amino acid substitutions occurred in the four other potential Kcv Ser/Thr phosphorylation sites at residues 40, 49, 59, and 60 (Fig. 3*A*).

An amino acid alignment of the seven proteins together with a schematic representation of channel domains based on the bacterial channel KcsA (5, 9) is shown in Fig. 3*A*. In summary, these results indicate that the *kcv* gene is widespread in viruses that infect *Chlorella NC64A*. Furthermore, many nucleotide substitutions that produce significant amino acid changes in the Kcv protein occur in the viral *kcv* genes.

Inhibitors of Virus Plaque Formation. Previous experiments established that PBCV-1 *kcv* expression in *Xenopus* oocytes, as well as

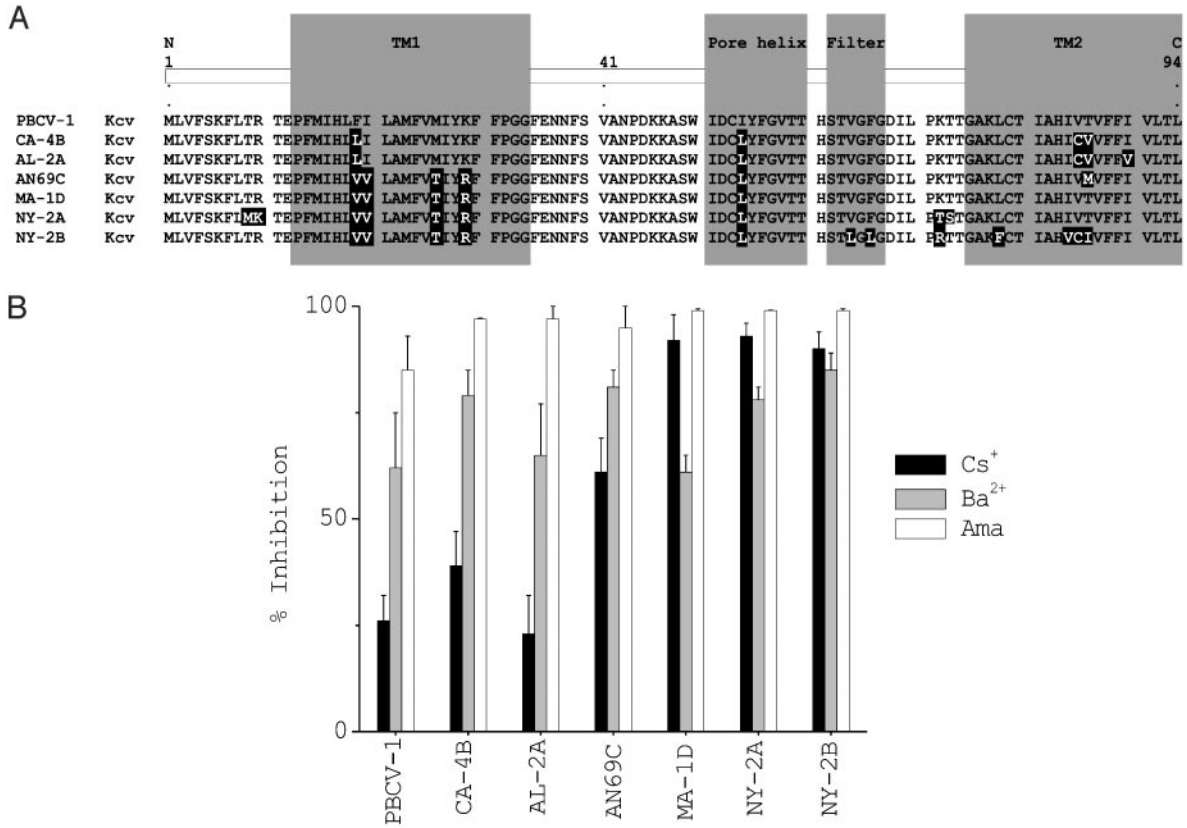

Fig. 3. Diversity of Kcv proteins and sensitivity of corresponding viruses to channel inhibitors. (*A*) Alignment of the seven different Kcv proteins. Each protein is named after a virus representative from each group. Amino acid substitutions, compared to PBCV-1 Kcv, are highlighted in black. The assignment of putative structure domains is based on an alignment with PBCV-1 Kcv and KcsA (5). TM1 and TM2, outer and inner transmembrane domains, respectively. (*B*) Plaque inhibition of chlorella viruses by potassium channel inhibitors amantadine, barium, and cesium.

PBCV-1 plaque formation (3), are sensitive to the K^+ channel inhibitors amantadine and Ba^{++} and less sensitive to Cs^+. We therefore tested the effect of these three inhibitors on viruses encoding each of the six Kcv-like proteins (Fig. 3*B*). The number of plaques produced by each of the viruses was inhibited 85% or more by 3 mM amantadine and 60% or more by 3 mM Ba^{++}. The sensitivity to 3 mM Cs^+ varied. Plaque formation by viruses PBCV-1, AL-2A, and CA-4B were partially resistant to 3 mM Cs^+ (20–40% inhibition); in contrast, 3 mM Cs^+ reduced plaque formation of AN69C by >70% and MA-1D, NY-2A, and NY-2B by ≥90% (Fig. 3*B*). None of these inhibitors affected the growth of the host chlorella at the concentrations tested and under the conditions used.

Expression in *Xenopus* Oocytes. We expressed the six Kcv-like proteins, along with PBCV-1 Kcv, in *Xenopus* oocytes to determine whether they produced functional K^+ channels. Oocytes were injected with the cRNAs, and a standard clamp protocol was applied to measure channel properties such as ion selectivity, voltage dependence of gating, and sensitivity to Ba^{++} and Cs^+. Fig. 4 shows currents recorded in a 50 mM KCl solution from oocytes injected with water as a control or with cRNA from PBCV-1 Kcv and the six new channels. All six Kcv-like proteins, as well as PBCV-1 Kcv, produced currents that differed from those of water-injected oocytes. However, the level of expression varied, ranging from ≤0.5 μA for CA-4B Kcv to ≥20 μA for MA-1D Kcv (at +80 mV).

Typically, the standard protocol evoked an instantaneous current (Ii) with a slope conductance approximately linear in the range −50 to +50 mV for all channels. Superimposed on this instantaneous component is a small time- and voltage-dependent component (It). The steady-state current measured at the end of the voltage step represents the sum of Ii and It. The corresponding instantaneous and steady-state current/voltage (*I–V*) relations of each channel are plotted to the right of each figure.

The current properties and *I–V* relations of the six Kcv-like channels differ significantly from those of PBCV-1 Kcv. The most obvious difference is the kinetics of the time-dependent component, which differs from that of PBCV-1 Kcv in all Kcv-like channels, decreasing at negative and increasing at positive voltages. As a result, at negative voltages, the instantaneous component is always larger than the steady-state component in Kcv-like channels. This is confirmed by the data reported in Table 1, which show the mean values for Ii and steady-state current (Iss) and their ratios. The value of Ii/Iss is <1 for PBCV-1 Kcv and >1 for all the other channels.

Kcv-Like Channels Inactivate at Negative Voltages in External K^+. In all Kcv-like channels, gating kinetics differed from those of PBCV-1 Kcv. Particularly evident was a very slow kinetic component of tail currents that did not reach steady state in our experimental protocol (tails collected at −80mV). In the example of Fig. 5, tail currents recorded at −80 mV after stepping to the range −150 to +70 mV are shown for PBCV-1 Kcv (Fig. 5*A*) and NY-2B Kcv (Fig. 5*B*). Whereas PBCV-1 Kcv tails displayed monophasic activation/deactivation (for test voltages more positive/negative than −80 mV, respectively), NY-2B tails displayed a biphasic time course (for test voltages more positive than −80 mV), implying the presence of an inactivation process.

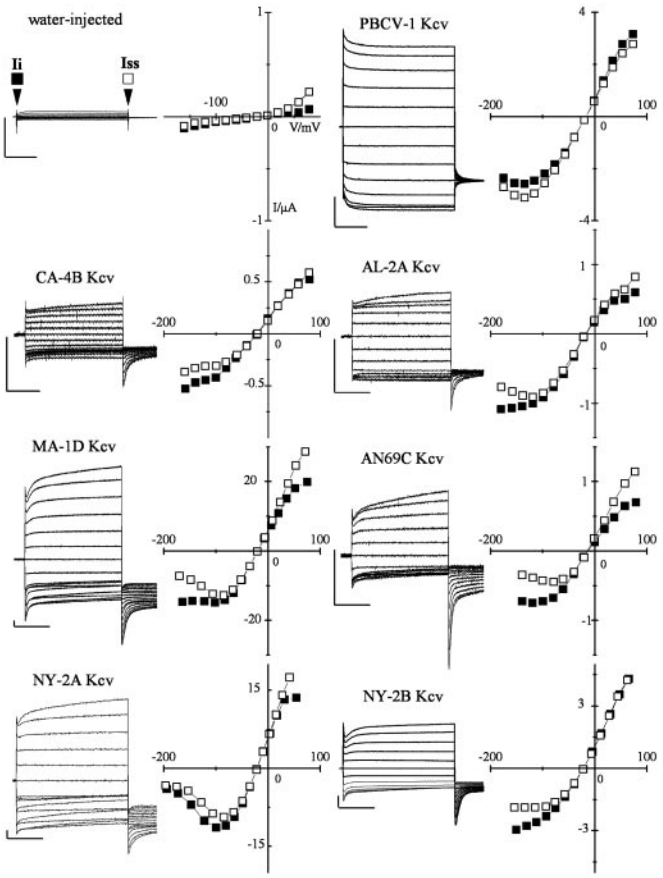

Fig. 4. All Kcv variants form functional K^+ channels in *Xenopus* oocytes. Expression of PBCV-1 Kcv and the six Kcv-like channels in *Xenopus* oocytes. Currents were recorded in 50 mM KCl from a representative oocyte injected either with water or with the cRNA of the indicated protein. Standard voltage protocol was: holding potential, –20 mV; steps of –20 mV from +80 mV to ≤−160 mV; postpotential, −80 mV. The corresponding *I–V* relation (*Right*) shows the instantaneous (Ii, ■) and the steady-state (Iss, □) currents, sampled at the beginning and end of the voltage pulse, as indicated by arrows in the water-injected sample. Vertical bar, 1 μA; horizontal bar, 200 ms.

As indicated by the activation curves of the time-dependent components (Fig. 5 *C* and *D*), a fraction of PBCV-1 Kcv channels open on hyperpolarization (19). In the example of Fig. 5*A*, the half-activation voltage (x_0) was −62.5 mV, and the inverse slope factor (dx) was 39.2 mV (mean ± SE; x_0 was −78 ± 13 mV, dx = 38 ± 9 mV, n = 7). In contrast, a fraction of NY-2B channels open and then inactivate on hyperpolarization. In the oocyte of Fig. 5*B*, fitting with the Boltzmann equation yielded x_0 = + 53.2 mV, dx = −35 mV (mean ± SE, x_0 was + 41.8 ± 7.7 mV, and dx = −31.7 ± 3.7 mV, n = 6) for the inactivation curve. Compared to the reference channel PBCV-1 Kcv, an inverted voltage dependence also occurred for Kcv from the other viruses (CA-4B, AL-2A, AN69C, MA-1D, and NY-2A). Half-maximum activation voltages were always positive and ranged from +30 mV (CA-4B Kcv) to +78 mV (NY-2A Kcv); inverse slope factors were always <−30 mV.

Table 1. Mean values of instantaneous (Ii) and steady-state (Iss) currents of the seven Kcv channels measured at −140 mV

Channel	Ii	Iss	Ii/Iss
PBCV-1 Kcv	1.09 ± 0.05 (n = 4)	1.13 ± 0.04 (n = 4)	0.96
CA-4B Kcv	1.31 ± 0.06 (n = 3)	1.24 ± 0.04 (n = 3)	1.06
AL-2A Kcv	1.36 ± ND (n = 2)	1.27 ± ND (n = 2)	1.07
AN69C Kcv	0.91 ± 0.04 (n = 3)	0.87 ± 0.03 (n = 3)	1.05
MA-1D Kcv	0.98 ± 0.03 (n = 4)	0.82 ± 0.03 (n = 4)	1.19
NY-2A Kcv	0.74 ± 0.04 (n = 5)	0.67 ± 0.09 (n = 5)	1.10
NY-2B Kcv	1.15 ± 0.03 (n = 5)	1.10 ± 0.10 (n = 5)	1.04

To overcome variability of expression between different oocytes and different channels, data have been normalized to the current values recorded at −100 mV.

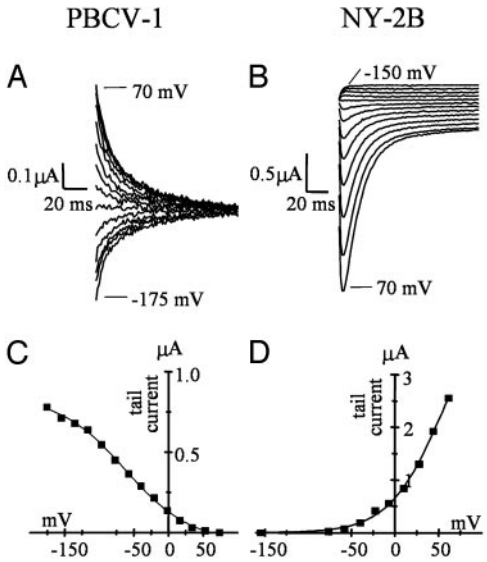

Fig. 5. Currents conducted by Kcv variants exhibit different kinetics. Shown is tail current analysis of PBCV-1 Kcv (*A*) and NY-2B Kcv (*B*), enlargement of the tail currents of PBCV-1 Kcv and NY-2B Kcv from Fig. 4. Tail currents were collected at −80 mV after stepping to test voltages between the indicated values. (*C* and *D*) Activation curves obtained from the tail current values (after subtraction of the time-independent current component) plotted against the conditioning voltages. Data were fitted with a Boltzmann-derived equation, $Y = A1–A2/(1 + \exp((x-x_0)/dx))) + A2$. The value for half-maximum activation, x_0, is −62.5 mV for PBCV-1 Kcv (*C*) and 53.2 mV for NY-2B (*D*). The inverse slope factor, dx, is 39.2 mV for PBCV-1 Kcv and −35 mV for NY-2B.

Permeability Properties of Kcv Channels. We examined the permeabilities of PBCV-1 Kcv and three Kcv-like channels to monovalent cations. Permeability ratios (P_{X+}/P_{K+}, X^+ = Rb^+, K^+, Cs^+, Na^+, Li^+, in that order) were: PBCV-1 Kcv, 1.07, 1, 0.52, 0.43, and 0.33; MA-1D Kcv, 1.11, 1, 0.41, 0.31, and 0.32; NY-2A Kcv, 1.16, 1, 0.77, 0.36, and 0.36; and NY-2B Kcv, 1.15, 1, 0.68, 0.27, and 0.35.

PBCV-1 Kcv shows a type III selectivity sequence $Rb^+ > K^+ > Cs^+ > Na^+ > Li^+$ (16), and the Kcv-like channels have similar cation selectivities with the exception of permeabilities to Na^+ and Li^+. The general similarity in selectivity among all of the Kcv channels is surprising particularly for NY-2B Kcv, because it has two amino acid substitutions in its selectivity filter (lGLG).

Rb^+ Affects Current Kinetics. In several cases, channel conductance depended on the permeating ion species. The most dramatic effect was observed when K^+ was replaced with Rb^+. Fig. 6 shows sample currents from oocytes expressing PBCV-1 Kcv (*Upper*) or NY-2A Kcv (*Lower*). In PBCV-1 Kcv, Rb^+ evoked a fast time-dependent inhibition of the inward current. The *I–V* relation showed a marked reduction of the steady-state current in Rb^+ solution at negative voltages reflecting the voltage-dependent block of the inward current. In contrast, replacing K^+ with Rb^+ resulted in an increase of the inward current in NY-2A Kcv (Fig. 6 *Lower*). Also, the inactivation process observed in the

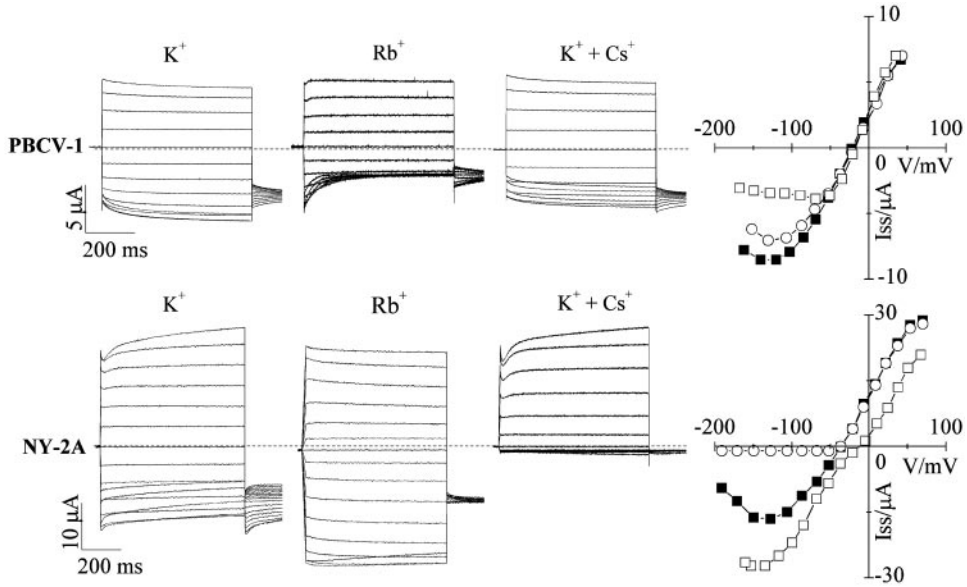

Fig. 6. Kcv variants show different cation dependencies. Shown is a comparison of current properties of PBCV-1 Kcv (*Upper*) and NY-2A Kcv (*Lower*) in the presence of different cations. First column, reference currents recorded in K^+. Second column, opposite effects of Rb^+ on the kinetics and the inward current. Third column, different degrees of voltage-dependent inhibition of K^+ current by Cs^+. Fourth column, *I–V* plots reporting steady-state currents (■) 50 mM K^+, (□) 50 mM Rb^+, (○) 50 mM K^+ + 10 mM Cs^+. Standard voltage protocol is as in Fig. 4.

inward K^+ currents was almost absent when the current was carried by Rb^+ and, notably, current kinetics of NY-2A Kcv in Rb^+ solutions were similar to those of PBCV-1 Kcv in K^+ solutions. The reversal potential of the current underwent a small shift to more positive voltages, indicating that the channel conducts Rb^+ slightly better than K^+. We observed an increase in the inward current in Rb^+ solutions and an absence of inactivation in all of the other Kcv-like channels, with the exception of NY-2B Kcv. NY-2B behaved like PBCV-1 Kcv showing a strong inhibition of the inward currents in Rb^+ solutions (results not shown).

Block by Cs^+. As reported previously (3), PBCV-1 plaque formation is not very sensitive to Cs^+ (≈26% inhibition, Fig. 3*B*). In contrast, plaque formation of viruses AN69C, MA-1D, NY-2B, and NY-2A is strongly inhibited by Cs^+. We therefore examined the effect of Cs^+ on the K^+ conductance of the corresponding Kcv channels. Fig. 6 compares the effect of 10 mM Cs^+ added to a solution of 50 mM K^+ on PBCV-1 Kcv and NY-2A Kcv. PBCV-1 Kcv current was slightly reduced by Cs^+ at voltages more negative than −80 mV (14% at –100 mV). In contrast, the NY-2A inward current was completely blocked by Cs^+. From dose–response curves (results not shown), we calculated a K_i of 0.1 mM at –100 mV for NY-2A Kcv. Cs^+ also completely inhibited K^+ inward currents in AN69C Kcv, MA-1D Kcv, and NY-2B Kcv (results not shown). Collectively, the Cs^+ sensitivity of the different viruses found in the plaque assays (Fig. 3*B*) correlates with the Cs^+ sensitivity of their Kcv channels.

Discussion

The results presented here demonstrate that variants of the *kcv* gene encoding a K^+ channel protein are ubiquitous in viruses that infect *Chlorella NC64A*. Previous studies (3) indicate that virus PBCV-1 replication is inhibited by the same compounds (amantadine and Ba^{++} but not Cs^+) that inhibit Kcv channel activity in oocytes, suggesting that the channel is important for viral replication. The present experiments provide additional support for this hypothesis, because some of the Kcv channel variants are more sensitive to Cs^+ than PBCV-1 Kcv. Plaque formation of viruses containing Kcv channels with increased Cs^+ sensitivity is also strongly inhibited by Cs^+. However, the function(s) of the Kcv channel in chlorella virus replication is unknown.

Sequence analyses of the *kcv* gene from 40 chlorella viruses identified 74 nucleotide substitutions of the 285 nucleotides in the genes. Collectively, these nucleotide substitutions produced six new Kcv proteins with 16 amino acid substitutions in the 94-aa protein. Substitutions occurred in all functional domains of the channel (N terminus, TM1, pore helix, selectivity filter, and TM2), with the exception of the extracellular loop (turret).

Each of the six Kcv-like proteins produced a K^+ selective conductance in *Xenopus* oocytes. The similarity in ion selectivity among all of the Kcv channels is surprising, particularly for virus NY-2B-Kcv. Although all other chlorella virus channels have the conserved pore motif "G(F/Y)G" characteristic of K^+ channels, the NY-2B Kcv channel has a "GLG" motif in the selectivity filter. A GLG motif occurs in the second pore domain of some "two-pore" channels like TWIK-1 and -2 (20, 21). However, NY-2B Kcv is unique among "one-pore" channels. Although similar in terms of ion selectivity and sensitivity to Ba^{++}, the Kcv-like channels differ with respect to Cs^+ sensitivity, kinetics, and cation dependency.

Alignment of the seven channels (Fig. 3*A*) highlights common amino acid substitutions, which could correlate with the above properties. Compared to PBCV-1 Kcv, all Kcv-like channels have two amino acid substitutions, in positions 19 and 54, localized in TM1 and the pore helix, respectively. These substitutions might be related to the inactivation of inward currents in K^+, a property shared by all of them. Channels that do not show inactivation of inward current in Rb^+ (all Kcv-like channels except for NY-2B) have several conserved residue combinations that are absent in PBCV-1 and NY-2B (Leu-54-Val-64; Leu-54-Phe-66; Leu-54-Leu-78, and Leu-54–Ileu84). The combination Leu-54–Phe-66 in the pore helix and selectivity filter is especially intriguing, given the important role of Phe-66 in the control of ion permeability in K^+ channels. Finally, channels that are completely blocked by Cs^+ (AN69C, MA-1D, NY-2A, and NY-2B Kcvs) have three common amino acid substitutions in TM1, Val-20, Thr-26, and Arg-29.

Channels from viruses MA-1D and PBCV-1 differ by five amino acids, and single site-directed mutation analysis has already established that the functional differences between the two channels cannot be explained by single amino acid substitutions (data not shown). To examine the functional relevance of the amino acid combinations mentioned above, combinatory site-directed amino acid mutations will be made to change the

reference channel PBCV-1 Kcv into one of the new channels and vice versa.

In summary, all six Kcv-like proteins form functional K^+-selective channels and exhibit different biophysical features, including altered kinetics and inhibition by Cs^+. The amino acid substitutions, together with the different properties found in these Kcv channels, will be used to guide site-directed mutations, either singularly or in combination, to identify key amino acids involved in conferring specific properties to Kcv. Finally, the chlorella viruses provide an apparently unlimited source of K^+ channel proteins with amino acid substitutions that can be used for structure–function studies.

We thank Mike Graves (University of Nebraska, Lincoln) and Yuanzheng Zhang (University of Nebraska, Lincoln) for many suggestions and Jack Dainty (University of East Anglia, Norwich, U.K.), Dan Minor (University of California, San Francisco), and Mauricio Montal (University of California at San Diego, La Jolla) for reading the manuscript and helpful discussions. This investigation was supported, in part, by Public Health Service Grant GM32441 (to J.L.V.E.) and National Institutes of Health Grant P20 RR15635 from the Centers of Biomedical Research Excellence Program of the National Center for Research Resources (to J.L.V.E.). G.T. was supported by the Deutsche Forschungsgemeinschaft, and A.M. was supported by Ministero Istruzione Università e Ricerca, Progetto Fondo per gli Investimenti della Ricerca di Base.

1. Van Etten, J. L. & Meints, R. H. (1999) *Annu. Rev. Microbiol.* **53,** 447–494.
2. Van Etten, J. L. (2003) *Annu. Rev. Genet.* **37,** 153–195.
3. Plugge, B., Gazzarrini, S., Nelson, M., Cerana, R., Van Etten, J. L., Derst, C., DiFrancesco, D., Moroni, A. & Thiel, G. (2000) *Science* **287,** 1641–1644.
4. Moroni, A., Viscomi, C., Sangiorgio, V., Pagliuca, C., Meckel, T., Horvath, F., Gazzarrini, S., Valbuzzi, P., Van Etten, J. L., DiFrancesco, D. & Thiel, G. (2002) *FEBS Lett.* **530,** 65–69.
5. Gazzarrini, S., Severino, M., Lombardi, M., Morandi, M., DiFrancesco, D., Van Etten, J., Thiel, G. & Moroni, A. (2003) *FEBS Lett.* **552,** 12–16.
6. Heginbotham, L., Lu, Z., Abramson, T. & MacKinnon, R. (1994) *Biophys. J.* **66,** 1061–1067.
7. Yifrach, O. & MacKinnon, R. (2002) *Cell* **111,** 231–239.
8. Minor, D. L., Jr., Masseling, S. J., Jan, Y. N. & Jan, L. Y. (1999) *Cell* **96,** 879–891.
9. Doyle, D. A., Cabral, J. M., Pfuetzner, R.-A., Kuo, A., Gulbis, J. M., Cohen, S. L., Chait, B. T. & MacKinnon, R. (1998) *Science* **280,** 69–76.
10. Kuo, A., Gulbis, J. M., Antcliff, J. F., Rahman, T., Lowe, E. D., Zimmer, J., Cuthbertson, J., Ashcroft, F. M., Ezaki, T. & Doyle, D. A. (2003) *Science* **300,** 1922–1926.
11. Mehmel, M., Rothermel, M., Meckel, T., Van Etten, J. L., Moroni, A. & Thiel, G. (2003) *FEBS Lett.* **552,** 7–11.
12. Villarreal, L. P. & DeFilippis, V. R. (2000) *J. Virol.* **74,** 7079–7084.
13. Van Etten, J. L., Meints, R. H., Burbank, D. C., Kuczmarski, D., Cuppels, D. A. & Lane, L. C. (1981) *Virology* **113,** 704–711.
14. Van Etten, J. L., Burbank, D. E., Kuczmarski, D. & Meints, R. H. (1983) *Science* **219,** 994–996.
15. Van Etten, J. L., Burbank, D. E., Xia, Y. & Meints, R. H. (1983) *Virology* **126,** 117–125.
16. Hille, B. (2001) *Ion Channels of Excitable Membranes* (Sinauer, Sunderland, MS), 3rd Ed.
17. Graves, M. V., Bernadt, C. T., Cerny, R. & Van Etten, J. L. (2001) *Virology* **285,** 332–345.
18. Sun, L., Li, Y., McCullough, A. K., Wood, T. G., Lloyd, R. S., Adams, B., Gurnon, J. R. & Van Etten, J. L. (2000) *J. Mol. Evol.* **50,** 82–92.
19. Gazzarrini, S., Van Etten, J. L., DiFrancesco, D., Thiel, G. & Moroni, A. (2002) *J. Membr. Biol.* **187,** 15–25.
20. Lesage, F., Guillemare, E., Fink, M., Duprat, F., Lazdunski, M., Romey, G. & Barhanin, J. (1996) *J. Biol. Chem.* **271,** 4183–4187.
21. Patel, A. J., Maingret, F., Magnone, V., Fosset, M., Lazdunski, M. & Honore, E. (2000) *J. Biol. Chem.* **275,** 28722–28730.